Treatment of Multiple Brain Metastases Using Stereotactic Radiosurgery with Single-Isocenter Volumetric Modulated Arc Therapy: Comparison with Conventional Dynamic Conformal Arc and Static Beam Stereotactic Radiosurgery

by

Chi Huang

Graduate Program in Medical Physics
Duke University

Date: _____

Approved:

_____
Zhiheng Wang, Supervisor

_____
Lei Ren

_____
Robert Reiman

Thesis submitted in partial fulfillment of the requirements for the degree of
Master of Science in the Graduate Program in Medical Physics
in the Graduate School of Duke University
2012

ABSTRACT

Treatment of Multiple Brain Metastases Using Stereotactic Radiosurgery with Single-Isocenter Volumetric Modulated Arc Therapy: Comparison with Conventional Dynamic Conformal Arc and Static Beam Stereotactic Radiosurgery

by

Chi Huang

Graduate Program in Medical Physics
Duke University

Date: _____

Approved:

_____
Zhiheng Wang, Supervisor

_____
Lei Ren

_____
Robert Reiman

An abstract of a thesis submitted in partial fulfillment of the requirements for the degree of Master of Science in the Graduate Program in Medical Physics in the Graduate School of Duke University
2012

Abstract

Both dynamic conformal arc therapy (DCAT) and three-dimensional conformal radiation therapy (3D-CRT) are well-established techniques and have commonly been used for stereotactic radiosurgery (SRS) treatment in brain metastases. However, for multiple metastases, a much longer treatment time results from multi-isocenter setup in DCAT and 3D-CRT. The aim of this study is to investigate the treatment of multiple brain metastases using single-isocenter volumetric modulated arc therapy (VMAT) compared with conventional multi-isocenter DCAT and 3D-CRT.

A series of 17 patients with 2 to 5 brain metastatic lesions were studied. For patients treated with DCAT/3D-CRT plans, VMAT plans were retrospectively generated, and vice versa. The number of isocenters was proportional to the number of PTVs in DCAT/3D-CRT plans while single-isocenter was employed in VMAT plans. The DCAT/3D-CRT and VMAT plans were generated using BrainLAB iPlan® RT Dose v4.1.1 and Varian Eclipse™ v8.6 treatment planning system, respectively. All plans were designed to be delivered on Novalis Tx™ system.

Conformity for VMAT plans was equivalent to or better than that for DCAT/3D-CRT plans. VMAT and DCAT/3D-CRT plans have similar target coverage, and VMAT plans have higher quality of coverage. However, the mean increase of 46% in the volume of low-dose region receiving 5 Gy was observed in VMAT plans. In addition, the distance between individual PTVs and VMAT isocenter has no impact on VMAT plans. The mean monitor units (MU) decreased by 42% and the mean treatment time decreased by 49% for VMAT plans.

This work suggests that single-isocenter VMAT is promising for SRS in the treatment of multiple brain metastases. Single-isocenter VMAT is able to achieve comparable dose conformity, target coverage, and quality of coverage to conventional DCAT and 3D-CRT plans with significantly superior delivery efficiency. However, single-isocenter VMAT might result in a larger low-dose region.

Contents

Abstract iv

List of Tables vii

List of Figures viii

Acknowledgements ix

1 Introduction and Background 1

1.1 Brain Metastases 1

1.2 Stereotactic Radiosurgery 2

1.3 Techniques for LINAC-Based SRS 5

1.3.1 Circular Arc Technique 6

1.3.2 Three-Dimensional Conformal Radiation Therapy 6

1.3.3 Dynamic Conformal Arc Therapy 7

1.3.4 Intensity Modulated Radiation Therapy 7

1.3.5 Volumetric Modulated Arc Therapy 8

1.4 Aims 9

2 Methods and Materials 11

2.1 Patient Selection 11

2.2 Equipment 12

2.3 Treatment Planning 12

2.3.1 DCAT and 3D-CRT Treatment Planning 13

2.3.2 VMAT Treatment Planning 14

2.4 Plan Evaluation 15

2.4.1 Conformity Index, Target Coverage, and Quality of Coverage 15

2.4.2 Normal Tissue Receiving Low Dose 17

2.4.3 Treatment Delivery Efficiency 17

2.5 Impact of the Distance Between Individual PTVs and VMAT Isocenter 19

3 Results 20

3.1 Dose Conformity, Target Coverage, and Quality of Coverage 20

3.2 Normal Tissue Receiving Low Dose 29

3.3 Treatment Delivery Efficiency 32

3.4 Impact of the Distance Between Individual PTVs and VMAT Isocenter 34

4 Discussion 35

5 Conclusion 38

Bibliography 39

List of Tables

Table 2-1: PTV volume (cm^3) and prescription doses (Gy) in 17 patients. 11

Table 3-1: Comparison of dosimetric parameters for patients with 5 lesions. 21

Table 3-2: Comparison of dosimetric parameters for patients with 4 lesions. 23

Table 3-3: Comparison of dosimetric parameters for patients with 3 lesions. 25

Table 3-4: Comparison of dosimetric parameters for patients with 2 lesions. 27

Table 3-5: Comparison of mean dosimetric parameters between DCAT/3D-CRT and VMAT plans in 17 patients with different numbers of lesions. The highlighted p value indicates a significant difference. 29

Table 3-6: The volume of the low-dose region for DCAT/3D-CRT and VMAT plans. The low-dose region is defined as the volume receiving a dose of 5 Gy or greater. The values for VMAT plans were normalized to DCAT/3D-CRT plans and expressed in percentages. 30

Table 3-7: The monitor units and treatment time for DCAT/3D-CRT and VMAT plans. The values of monitor unit and treatment time for VMAT plans were normalized to DCAT/3D-CRT plans and expressed in percentages. 32

Table 3-8: Comparison of dosimetric parameters for a total of 59 PTVs in the central and peripheral group between DCAT/3D-CRT and VMAT plans. The highlighted p value indicates a significant difference..... 34

List of Figures

Figure 2-1: Definition of the volumes used in conformity and coverage parameters. Solid line is the target volume, V_T; dotted line is the prescription isodose, pi; shaded area is the volume encompassed by the prescription isodose, V_{pi}; and hatched area is the target volume encompassed by the prescription isodose, $V_{T,pi}$. (Redrawn from N. J. Lomax and S. G. Scheib, Qualifying the degree of conformity in radiosurgery treatment planning. *Int J Radiat Oncol Biol Phys* 2003, 55(5):1409-19). 17

Figure 3-1: (A) Conformity index, (B) target coverage, and (C) quality of coverage for DCAT/3D-CRT and VMAT plans in patients with 5 lesions. 22

Figure 3-2: (A) Conformity index, (B) target coverage, and (C) quality of coverage for DCAT/3D-CRT and VMAT plans in patients with 4 lesions. 24

Figure 3-3: (A) Conformity index, (B) target coverage, and (C) quality of coverage for DCAT/3D-CRT and VMAT plans in patients with 3 lesions. 26

Figure 3-4: (A) Conformity index, (B) target coverage, and (C) quality of coverage for DCAT/3D-CRT and VMAT plans in patients with 2 lesions. 28

Figure 3-5: The volume of the low-dose region (volume receiving 5 Gy) for DCAT/3D-CRT and VMAT plans. 30

Figure 3-6: Isodose distributions for a patient with 5 lesions in DCAT/3D-CRT plans (left) and VMAT plans (right). The blue isodose lines are 5 Gy. 31

Figure 3-7: The monitor units for DCAT/3D-CRT and VMAT plans. 33

Figure 3-8: The treatment time for DCAT/3D-CRT and VMAT plans. 33

Figure 4-1: Illustration of pitch, roll, and yaw rotations. Rotation about x axis is pitch; rotation about y axis is roll; rotation about z axis is yaw. 37

Acknowledgements

I would like to thank my advisor, Dr. Zhiheng Wang, for his insight, guidance, patience, and encouragement throughout this project. I would also like to express my gratitude to Dr. Ren Lei and Dr. Robert Reiman for serving on my committee and sharing their knowledge with me. Finally, I am thankful to my family and friends for their unconditional support.

1

Introduction and Background

1.1 Brain Metastases

Brain metastases are the most common intracranial neoplasm in adults. It is estimated that 8-10% of adults with cancer will develop symptomatic brain metastases during their lives, and the approximate annual incidence is 200,000 in the U.S. The majority of brain metastases originate from primary cancers in the lung, kidney, breast, colon, and skin (melanoma) [1]. Approximately over 50% of patients present with multiple metastases, which are seen more frequently with lung cancer and melanoma. Brain metastases are a significant cause of morbidity and mortality in cancer patients. The median survival for patients who receive no treatment is 1 month [2, 3]. The frequency of diagnosis of brain metastases is increasing as advances in imaging modalities and earlier detection as well as longer survival because of better control of primary cancers [4].

Common therapeutic approaches to brain metastases include chemotherapy, surgery, whole brain radiation therapy (WBRT), stereotactic radiosurgery (SRS), and a combination of these therapies. While chemotherapy is suitable for some chemosensitive metastatic tumors, such as lymphoma and small cell lung cancer, the main concerns are the ability of chemotherapeutic agent to cross blood-brain barrier (BBB) and the uncertainty of the agent concentration delivered to the tumor. Benefits of surgery include rapid and reliable relief of neurological symptoms caused by mass effect and establishment of local control. However, surgical resection is invasive and is usually limited to patients with a dominant lesion. That is, only selected patients with

multiple metastases benefit from surgery. WBRT offers effective palliation of neurological symptoms for patients with multiple brain metastases that are intractable for surgery, but the long-term adverse effect on neurocognitive function, including dementia, cerebral atrophy, and difficulty with short-term memory and performing calculations, might not be negligible [3, 5, 6].

Brain metastases currently represent the most common indication for SRS. Equivalent outcomes in terms of local control and survival prolongation have been observed for patients with single metastasis amenable to either SRS or surgery. SRS may have superior local control for radioresistant lesions that are less responsive to WBRT such as renal cell and melanoma, and it allows a reduction or deferral of WBRT to be used as a later salvage treatment without possible adverse effects [2]. In addition to the treatment of newly diagnosed brain metastases, SRS is suitable for patients with recurrent or progressive brain metastases due to its limited treated volumes. The ability of treating more than one lesion in a single session makes SRS feasible to treat multiple brain metastases [2, 4-8].

1.2 Stereotactic Radiosurgery

Stereotactic radiosurgery (SRS) uses high dose of radiation in combination with stereotactic apparatus to irradiate intracranial lesions in a single fraction. Instead of exploiting higher radiosensitivity of lesions relative to normal tissue in the conventional fractionated radiation therapy, SRS takes the advantage of highly focused beam to acquire high degree of dose conformity and accuracy of beam delivery while spares dose to surrounding normal tissue. It is particularly useful for lesions which are inaccessible or unsuitable with other treatments such as surgery. The size of lesions plays an important role in SRS. Conventionally, patients with lesion less than 4 cm in diameter are generally considered candidates for SRS. Treatment of large lesions is compromised due to the need for lower prescription dose to prevent damage to surrounding normal tissue. The dose to normal tissue might exceed the acceptable limits when a

large lesion is treated in a single fraction. For single fraction SRS, the maximum tolerated doses of 24, 18, and 15 Gy have been established by the Radiation Therapy Oncology Group (RTOG) 90-05 protocol for lesions ≤ 20 mm, 21-30 mm, and 31-40 mm in maximum diameter, respectively [3, 9]. The majority of brain metastatic lesions have distinct pathologic and radiographic margins as well as a maximum diameter of less than 4 cm, making them ideal candidates for SRS [3].

SRS was first developed by Lars Leksell in 1951. The term "stereotactic" means accurate localization in three-dimensional coordinates during imaging acquisition and treatment delivery using stereotactic apparatus. Target location is accurately defined by the localization rods in the stereotactic frame in imaging studies, including computed tomography (CT), magnetic resonance imaging (MRI), angiography, and positron emission tomography (PET). The SRS approach generally evolves from invasive to non-invasive systems. SRS has traditionally been performed by fixing an invasive head ring to patient's skull with screws followed by attaching a stereotactic frame to the head ring. While the rigid fixation provides robust localization and minimizes head motion, it causes pain and discomfort. In addition, the placement of the head ring and patient setup are cumbersome and time-consuming, requiring an experienced oncology team to perform. The non-invasive stereotactic apparatus provides an alternative to SRS. Advances in image-guided systems allow the development of non-invasive systems, which typically employ a thermoplastic mask or a bite block with the aid of real-time image guidance during the treatment delivery and eliminate the use of the head ring. It also brings flexible treatment schemes, for example, hypofractionated radiosurgery [3, 10].

Common methods of delivering radiation in SRS treatment include Gamma Knife (GK), cyclotron, and linear accelerator (LINAC), which employ gamma rays, heavy charged particles, and high-energy photons, respectively. A GK consists of about 200 sources of cobalt-60 with cylindrical cones for beam collimation in a hemispheric helmet. High energy gamma rays from

the sources converge to a single focal point. The GK usually requires an invasive head ring for immobilization and localization, thus being limited to treatment in single fraction. Heavy charged particles such as protons and carbon ions deposit energy at certain depths, i.e., Bragg peak, minimizing the dose to surrounding normal tissue. However, more investigations are needed to justify the use of heavy charged particles for different diseases. In addition, both the size and the expense of cyclotron limit this delivery method to a few cancer centers [2, 3, 6, 11-13].

A number of megavoltage (MV) X-ray beams produced by the LINAC are able to shape small volumes of radiation as those created by the GK. The conventional LINAC with a C-arm gantry is available for radiation therapy in most of the oncology departments, thus being widely used for SRS treatment delivery nowadays. Most of the LINACs can be easily adapted for SRS. While the LINAC for routine external beam delivery employs a multileaf collimator (MLC), the LINAC for the use of SRS are equipped with special tertiary collimators such as cones and a micro-multileaf collimator (mMLC) to achieve more precise beam delivery and better definition for small fields. The collimated beams from the LINAC are focused on an intracranial target by rotating the gantry and couch with respect to one isocenter. In addition to the ability to conform tightly to the field, tertiary collimators are closer to the patient, reducing penumbra compared with jaws. LINAC-based SRS also enables non-invasive systems, making more treatment techniques available, such as fractionated stereotactic radiation therapy (FST) and extracranial radiosurgery [3, 13].

In addition to the conventional LINAC-based SRS delivery, which employs the existing LINAC with tertiary collimators, there are some modified LINAC-based SRS delivery units. The CyberKnife® (Accuray, USA) is a frameless system with real-time image guidance, delivering 6 MV photons through a lightweight LINAC mounted on a robotic arm with six degrees of freedom. Two ceiling-mounted diagnostic x-ray tubes with corresponding orthogonal, floor-mounted amorphous silicon detectors provide real-time imaging. In contrast to the conventional

LINAC-based SRS, which the misalignment is corrected by couch movement, the real-time image guidance enables tracking of target movement during treatment delivery followed by instantaneous beam positioning adjustment done by the robotic arm, which eliminates the need of the stereotactic frame. The use of robotic arm also allows non-isocentric beams through circular collimators of varying size, which conforms more closely to the targets. In addition, simultaneous irradiation of multiple lesions can be achieved by non-isocentric treatment [3, 14].

Another modified LINAC-based SRS delivery unit, the TomoTherapy® (Accuray, USA), employs LINAC mounted on a rotating ring gantry, which combines a delivery of 6 MV photons in a helical fashion with CT imaging capability. The TomoTherapy has integrated on-board imaging capability using lower energy (3.5 MV) beams. The intensity of the fan beams are modulated by 64 individual binary collimators across the axial plane. During the delivery, continuous and synchronous couch/patient travel through the bore with gantry rotation form a helical trajectory around the patient, which is similar to a CT scanner [3, 15].

1.3 Techniques for LINAC-Based SRS

This study focuses on an investigation of different techniques of conventional LINAC-based SRS, so common techniques for conventional LINCA-based SRS are discussed. Tertiary collimators, including circular cones and mMLC, are exploited in these techniques to shape small fields.

Early developments of LINAC-based SRS were focused on delivering beams through circular cones. Circular beams offer advantages over rectangular beams, including the sharper beam, easier dosimetry calculation, more precise beam delivery, and better field definition for small lesions [3]. However, to achieve adequate dose conformity for large or irregular lesions, multiple isocenters with overlapping fields are required, resulting in dose inhomogeneity and longer treatment time.

Though a MLC is able to shape irregular fields by moving leaves, the large projected width

at the isocenter and the penumbra prevent its use in SRS. The need of treating lesions with complex shapes is fulfilled by the introduction of mMLC. The width of a projected leaf at the isocenter is less than that in conventional MLC, which provides adequate dose conformity in SRS. Since a larger field can be shaped by mMLC compared with the field created by circular cones, single isocenter can lead to an acceptable plan. On the other hand, an inferior conformity may appear in tiny lesions due to an insufficiently small field created by the mMLC leaves, which are of the same order of the targets [3].

1.3.1 Circular Arc Technique

Circular arc technique employs multiple noncoplanar arcs delivered with circular cones. The arcs are spread to form a spherical or ellipsoidal dose distribution similar to that of the GK. It is particularly useful to treat small lesions, which require high precision in target localization. In contrast, dose inhomogeneity and longer treatment time may result from the use of multiple isocenters for large and irregular lesions. However, compared with the GK, more choices of the cone sizes and the availability of larger cone sizes in circular arc technique for corresponding lesion sizes reduce the need for using multiple isocenters [3, 16]. At Duke University Medical Center, patients with trigeminal neuralgia are treated with circular arc technique due to the small size of the target.

1.3.2 Three-Dimensional Conformal Radiation Therapy

In three-dimensional conformal radiation therapy (3D-CRT), a number of static fields shaped by the availability of mMLC from different directions conform to the beam's-eye-view (BEV) projection of target. Due to the ability to shape a larger field by mMLC compared with the field created by cones in circular arc technique, a better dose homogeneity in a large lesion can be achieved with single isocenter in 3D-CRT. However, single isocenter with static fields may result

in less steep dose gradient at the edge of the target due to the larger and fewer beams, so a sufficient number of beams are required to achieve adequate dose conformity. An insufficient number of beams will also increase the dose to the surrounding normal tissue. Therefore, a compromise needs to be reached between the plan quality and efficiency. These issues prompted the development of use of arc-based technique and inverse planning [3, 17, 18].

1.3.3 Dynamic Conformal Arc Therapy

In dynamic conformal arc therapy (DCAT), the field continuously conforms to the BEV projection of the target during gantry rotation by dynamic mMLC. DCAT utilizes the advantages of arc-based delivery which spare dose to the surrounding normal tissue with homogeneous dose distribution, and employs conformal beams to achieve high dose conformity. In addition, DCAT significantly improves delivery efficiency in terms of monitor unit (MU) per target dose. However, for complicated cases, for example, a target surrounded by critical structures, DCAT might yield inferior sparing compared with intensity modulated radiation therapy (IMRT) [17-20].

1.3.4 Intensity Modulated Radiation Therapy

In intensity modulated radiation therapy (IMRT), a modulated intensity pattern is generated by summation of nonuniform fluence delivered through a number of static beam directions with inverse planning. Forward planning is a trial-and-error approach in which the planners change the parameters of the beams to achieve an optimal plan. In inverse planning, in addition to the number and beam arrangement, treatment criteria including dose-volume objectives and their corresponding priorities are also defined. During the optimization, each beam is divided into many beamlets, and the weights or intensities of those beamlets are adjusted to achieve the desired dose distribution to meet the criteria. IMRT improves dose conformity for lesions with

complex shapes by providing a sharp dose falloff at the edge of the target. However, more MU used in IMRT may result in a larger volume of normal tissue that is exposed to low dose. Patients with large or irregular lesions are usually treated with IMRT [3, 18, 21].

1.3.5 Volumetric Modulated Arc Therapy

Volumetric modulated arc therapy (VMAT) efficiently delivers dynamically modulated intensity pattern with arc-based delivery. VMAT is an advanced development of intensity modulated arc therapy (IMAT) proposed by Yu in 1995. IMAT is theoretically able to achieve high conformity by combining a large number of beam directions of arc-based delivery and inverse planning. However, leaf motion constraints are imposed on the plans to ensure both the accuracy and the efficiency of the delivery. A large travel distance of MLC between adjacent control points (gantry positions) is undesirable since it introduces errors and restricts continuous gantry rotation. This constraint reduces the quality of optimization. Though increasing control points can improve accuracy, it further restricts the optimization.

Otto [22] proposed VMAT, a new approach to plan optimization to solve the limitation in IMAT. In VMAT, MLC aperture shape, dose rate, and the speed of gantry rotation are continuously varied during the gantry rotation to achieve conformal dose distribution. VMAT optimization is similar to direct aperture optimization (DAO) [23], which incorporates the constraints placed by the MLC position and MU weights into the optimization, thus eliminating the need and uncertainties of a separate leaf-sequencing. VMAT proposed by Otto further employs progressive sampling algorithm to overcome the challenges that the leaf motion constraints degrade the optimization quality in IMAT technique by gradually increasing the number of samples during the optimization. While initial coarse sampling offers the optimization algorithm a large flexibility to achieve a desired fluence map, introduced samples improve the leaf motion accuracy as well as plan accuracy.

During the optimization, mechanical constraints and efficiency constraints are both imposed on MLC leaf positions and MU weights. The mechanical constraints only accept physically achievable MLC leaf positions and MU weights (e.g., overlapping of opposing leaves or negative MU are rejected). The efficiency constraints ensure continuous delivery. That is, maximum leaf displacement per degree of gantry rotation is constrained based on the maximum leaf motion speed and maximum gantry rotation speed. In addition, since deceleration of the gantry decrease delivery accuracy and therefore is undesirable, MU weights are also constrained to avoid changes of the speed of the gantry rotation.

The use of VMAT for brain metastases has been investigated in several studies. While Otto focused on single arc delivery in VMAT technique, several arcs were used in some of these studies to provide adequate conformity and coverage for complex and large targets. For single brain metastasis, Audet et al [24] found that VMAT with multiple noncoplanar arcs is able to achieve high conformity, especially for large or irregular lesions, and is suitable for a greater range of prescription doses. The treatment time can be significantly reduced in single arc delivery [25]. However, a larger low dose area may result from multi-arc delivery [24, 25]. Regarding multiple brain metastases, Wolff et al [25] demonstrated that single-isocenter VMAT with single arc is a feasible approach to treat intracranial targets in SRS with less treatment time, less MU, and better conformity compared with circular arc technique. Clark et al [8] showed that single-isocenter VMAT plans can achieve equivalent conformity compared with multi-isocenter VMAT plans when multiple brain metastases are treated with SRS.

1.4 Aims

Both DCAT and 3D-CRT are well-established techniques and have commonly been used for SRS treatment in brain metastases to date. However, for multiple metastases, a much longer treatment time results from multi-isocenter setup in DCAT and 3D-CRT plans. All lesions have their

respective isocenters and plans to be delivered, and the on-line imaging acquisition is required for each isocenter. Therefore, the treatment time increases as the number of lesions increases. We expect that single-isocenter VMAT is able to treat multiple brain metastases with less treatment time. On a single patient basis, faster treatments minimize intra-fraction internal organ motion and patient motion. It also allows more time for on-line imaging acquisition. In addition, faster treatments increase the daily patient volume of the medical service.

The aim of this study is to investigate whether the treatment of multiple brain metastases using SRS with single-isocenter VMAT provides comparable results to conventional DCAT and 3D-CRT in terms of dosimetric performance and treatment delivery efficiency. In addition, the impact of the distance between individual PTVs and VMAT isocenter was evaluated.

2

Methods and Materials

2.1 Patient Selection

A series of 17 patients with 2 to 5 brain metastatic lesions were studied. All the patients were previously treated using SRS with DCAT or VMAT plans at Duke University Medical Center. Among all the patients, 14 patients were treated with DCAT plans and 3 patients were treated with VMAT plans. The patients were grouped according to the number of lesions. The planning target volumes (PTV) and their corresponding prescription doses are summarized in Table 2-1.

Table 2-1: PTV volume (cm^3) and prescription doses (Gy) in 17 patients.

	Volume (cm^3) / Prescription dose (Gy)									
	Patient 1		Patient 2		Patient 3		Patient 4			
PTV 1	10.8	14	8.25	15	1.95	18	4.25	18		
PTV 2	5.03	14	1.22	15	1.3	20	0.85	20		
PTV 3	3.96	14	3.07	18	1.28	20	0.56	11		
PTV 4	3.84	14	1.2	16	1.12	18	0.37	20		
PTV 5	1.21	14	1.08	20	0.65	20	0.37	20		
	Patient 5		Patient 6		Patient 7		Patient 8		Patient 9	
PTV 1	1.08	15	5.53	18	2.94	18	4.73	12	6.82	25
PTV 2	0.83	18	3.92	18	1.85	18	2.44	10	3.63	25
PTV 3	0.66	18	1.66	24	1.03	18	1.56	12	1.28	25
PTV 4	0.42	18	0.6	9	1.02	18	1.49	9	0.73	25
	Patient 10		Patient 11		Patient 12		Patient 13			
PTV 1	5.32	16	1.38	20	9.11	15	3.59	16		
PTV 2	1	20	0.66	20	1.17	20	0.4	18		
PTV 3	0.7	20	0.11	20	0.46	20	0.31	18		
	Patient 14		Patient 15		Patient 16		Patient 17			
PTV 1	2.43	20	4.14	16	3.92	18	1.81	15		
PTV 2	0.33	20	0.5	15	1.07	20	1.3	20		

2.2 Equipment

The DCAT and 3D-CRT plans were generated using iPlan® RT Dose Version 4.1.1 (BrainLAB, Germany) treatment planning system. The dose distribution was calculated using pencil beam algorithm. The VMAT plans were generated using Eclipse™ Version 8.6 (Varian, USA) treatment planning system. The dose distribution was calculated using Anisotropic Analytical Algorithm Version 10.0.28 (Varian, USA).

All the plans were designed to be delivered on Novalis Tx™ system (Varian, USA and BrainLAB, Germany). The LINAC in Novalis Tx system is equipped with a high-definition 120 multileaf collimator (HD120® MLC). HD120 MLC consists of 60 pairs of leaves, including 32 pairs of 2.5 mm leaves in the central 8 cm and 14 pairs of 5 mm leaves on each side. The maximum leaf speed is 2.5 cm/s.

The patients were immobilized with U-Frame (BrainLAB, Germany) with imaging guidance systems. Novalis Tx system is equipped with imaging guidance systems, including on-board-imager® (OBI) with 2D and 3D kilovoltage (kV) imaging capabilities (Varian, USA) and ExacTrac® system (BrainLAB, Germany) which provides 6 degree-of-freedom kV imaging. ExacTrac system is able to correcting patient positioning rotationally though the robotic couch [12].

2.3 Treatment Planning

For patients treated with DCAT plans (patient 2-8, and 11-17), VMAT plans were retrospectively generated while for patients treated with VMAT plans (patient 1, 9, and 10), DCAT or 3D-CRT plans were retrospectively generated. Among those patients previously treated with VMAT plans, DCAT plans were generated for patient 1 and 10. For patient 9, a 3D-CRT plan instead of a DCAT plan was generated to obtain a more clinically acceptable plan. Since lesions in patient 9 were too

close to each other, the employment of discrete beam angles in 3D-CRT plans allows more flexibility in beam arrangement. However, a greater number of beams must be used to achieve dose conformity, which results in a longer treatment time.

DCAT/3D-CRT and VMAT plans were all designed to achieve conformal dose distribution while spare dose to surrounding normal tissue. The crucial distinction is that the number of isocenters was proportional to the number of PTVs in DCAT/3D-CRT plans while single-isocenter was employed in VMAT plans. The isocenters were placed at the center of each PTV and at the center of the union of PTVs for DCAT/3D-CRT and VMAT plans, respectively. In multi-isocenter planning e.g., DCAT and 3D-CRT plans, insufficient inter-isocenter spacing may result in a large dose inhomogeneity [26]. Therefore, lesions which are too close to each other are contoured as one PTV on which single isocenter is placed in clinical practice. In this study, PTV 1 and PTV 2 for patient 2 were too close to be separated, thus being treated and evaluated as a whole in both DCAT/3D-CRT and VMAT plans. The prescription doses for the retrospectively generated plans were identical to those for the previously treated plans given in Table 2-1.

2.3.1 DCAT and 3D-CRT Treatment Planning

DCAT treatment planning involves creating individual treatment group which consists of 3 to 5 non-coplanar conformal partial arcs for each PTV, followed by a summation of those treatment groups to get an overall dose distribution. 6 MV SRS photon beams and a dose rate of 1000 MU/min were used. To begin the planning, volume-dose prescription were specified and adjusted for each PTV. In individual treatment group, arcs were spread out to obtain higher dose homogeneity. Each arc which initially covered 100° to 120° was then adjusted to avoid passing beams through other PTVs and organs at risk (OAR) based on the BEV at any angles during the arc. In iPlan treatment planning system, HD120 MLC beam shaping conforms to the target every 10° along the arc path. If other PTVs or OARs were on the arc path, the arc length was shortened.

Collimators were adjusted to allow jaw motion along the short axis and a 2 mm of margin was expanded from the PTV to account for the penumbra of HD120 MLC. To achieve higher accuracy required for SRS, grid size in dose calculation was set as 1mm. The weighting of each arc were adjusted after dose calculation to achieve an optimal plan.

3D-CRT treatment planning generally followed a similar series of steps as that for DCAT treatment planning except for the fact that the conformal arcs were replaced by the conformal static beams. Instead of 3 to 5 conformal arcs, 9 to 11 conformal static beams were spread out for each PTV in individual treatment group, followed by a summation of these treatment groups. If it is hard to make a separation between beams and other PTVs because of the short distances at a certain beam angle, collimators were adjusted to cover the adjacent PTVs.

2.3.2 VMAT Treatment Planning

VMAT treatment planning involves focusing 3 to 5 partial arcs to a single isocenter at the center of the union of PTVs, which is defined as combined PTV. 6 MV SRS photon beams and a maximum dose rate of 600 MU/min were used. After arcs had been placed by designating the couch angles and gantry angles without the risk of collision, the jaw positions and collimator angles of each arc were adjusted to cover the combined PTV while spare dose to the surrounding normal tissue. The arc length was shortened if the beam was too close to the OARs. To minimize the impact of interleaf leakage, the collimator angles were set to non-zero values and adjusted to match the PTV position during rotation. Dose-volume objectives and their corresponding priorities for individual PTV and OARs were specified before VMAT optimization. A penalty region, a 3 cm expansion from the combined PTV, was contoured and incorporated into the optimization to reduce doses to normal tissue. After dose calculation, if the dose between adjacent PTVs was too high, additional penalty regions were manually contoured based on the dose distributions and incorporated into optimization.

2.4 Plan Evaluation

To compare the treatments with VMAT and DCAT/3D-CRT plans, quantitative parameters were selected as follows. For dosimetric evaluation, conformity index (CI), target coverage (TC), and quality of coverage for PTV were computed. The volume of normal tissue receiving a dose of 5 Gy or greater was recorded for the evaluation of low dose region. The significance of the difference in the mean values between VMAT and DCAT/3D-CRT plans were analyzed based on the paired t-test, in which a statistical significance was defined as $p < 0.05$. For delivery efficiency evaluation, the number of MU was also recorded to approximate the beam-on time and the total treatment time.

2.4.1 Conformity Index, Target Coverage, and Quality of Coverage

As modern radiation therapy pursues high dose conformity, which is also the primary goal of SRS, CI provides not only quantitative but also simplified information of the degree of agreement between isodoses, tumor contours, and normal tissue contours by geometric intersection methods for evaluation of plans. CI proposed by Radiation Therapy Oncology Group (RTOG) has been widely used for SRS evaluation, and it was employed in this study [27, 28]. CI_{RTOG} is defined as follows:

$$CI_{RTOG} = \frac{V_{pi}}{V_T} \tag{2.1}$$

where V_{pi} is the volume encompassed by the prescription isodose, and V_T is the target volume. An ideal value of CI_{RTOG} is 1. If the CI_{RTOG} is between 1 and 2, the plan is considered to comply with the protocol. CI_{RTOG} of VMAT plans was directly calculated by converting isodose to structure in Eclipse treatment planning system, and then divided by the target volume. On the other hand, iPlan has a different definition of CI as follows:

$$\mathrm{CI_{iPlan}} = 1 + \frac{\mathrm{V_{Normal,pi}}}{\mathrm{V_{T,pi}}} \tag{2.2}$$

where $V_{Normal,pi}$ is the volume of the normal tissue encompassed by the prescription isodose and $V_{T,pi}$ is the target volume encompassed by the prescription isodose. An ideal value of CI_{iPlan} is 1, which indicates no normal tissue receives prescription isodose. There is a small difference between CI_{RTOG} and CI_{iPlan} due to the high coverage in SRS. In order to make a fair comparison, CI_{RTOG} for DCAT/3D-CRT plans was computed based on the CI_{iPlan} by multiplying the target coverage (TC) as shown in Equation (2.3).

$$\mathrm{CI_{RTOG}} = \frac{\mathrm{V_{pi}}}{\mathrm{V_T}} = \frac{\mathrm{V_{T,pi}} + \mathrm{V_{Normal,pi}}}{\mathrm{V_T}} = \frac{\mathrm{V_{T,pi}} + \mathrm{V_{Normal,pi}}}{\mathrm{V_{T,pi}}} \times \frac{\mathrm{V_{T,pi}}}{\mathrm{V_T}} = \mathrm{CI_{iPlan}} \times \mathrm{TC} \tag{2.3}$$

Though CI has been frequently quoted in literature, CI alone does not take into account the location or the shape of isodose volume and target volume as shown in Figure 2-1, thus being inadequate for the evaluation of dose conformity [27]. Lomax et al. [28] claimed that CI along with the target coverage is a more useful tool. Target coverage (TC) expressed as a percentage is defined as follows:

$$\mathrm{TC} = \frac{\mathrm{V_{T,pi}}}{\mathrm{V_T}} \times 100\% \tag{2.4}$$

where $V_{T,pi}$ is the target volume encompassed by the prescription isodose. An ideal TC is 100%, and we aim to achieve a TC of 99% for each plan. Quality of coverage proposed by RTOG is defined as follows:

$$\text{Quality of coverage}_{\mathrm{RTOG}} = \frac{\mathrm{D_{min}}}{\mathrm{PI}} \tag{2.5}$$

where D_{min} is the minimum dose in the target, and PI is the prescription isodose. Quality of coverage stresses the importance of treating the whole target volume, and an ideal value is 1.

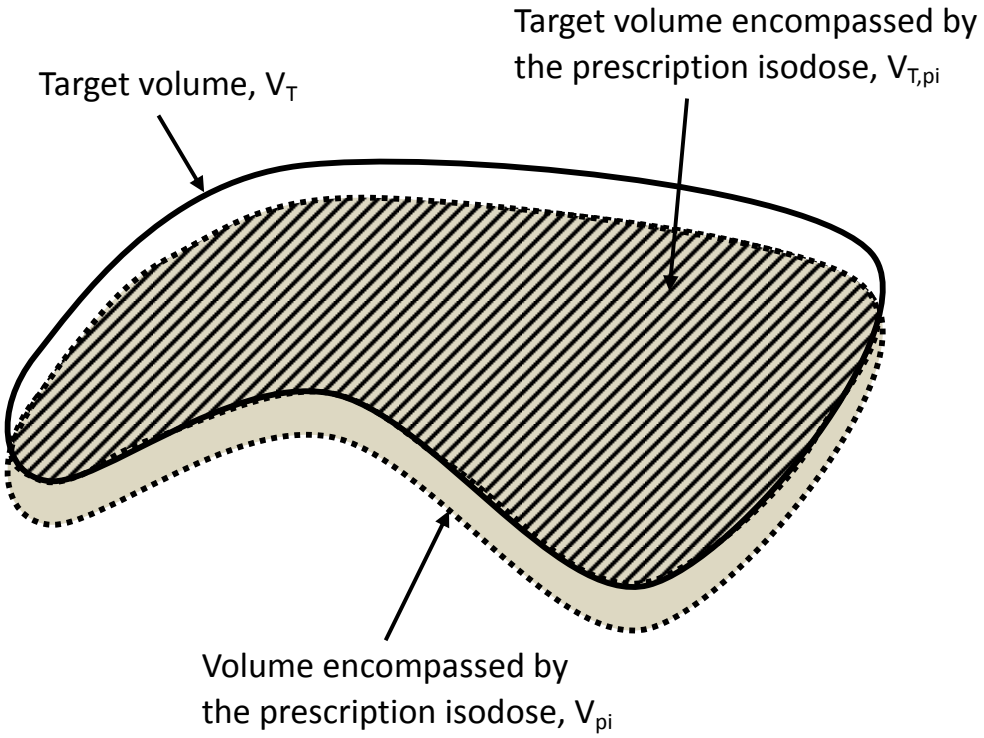

Figure 2-1: Definition of the volumes used in conformity and coverage parameters. Solid line is the target volume, V_T; dotted line is the prescription isodose, pi; shaded area is the volume encompassed by the prescription isodose, V_{pi}; and hatched area is the target volume encompassed by the prescription isodose, $V_{T,pi}$. (Redrawn from N. J. Lomax and S. G. Scheib, Qualifying the degree of conformity in radiosurgery treatment planning. *Int J Radiat Oncol Biol Phys* 2003, 55(5):1409-19).

2.4.2 Normal Tissue Receiving Low Dose

The volume of normal tissue receiving a dose of 5 Gy or greater is defined as the low-dose region. This volume shows the ability of the plans to spare dose to normal tissue, which may lead to complication or induce secondary malignancy.

2.4.3 Treatment Delivery Efficiency

Total treatment time, the sum of initial setup time, the time for on-line imaging acquisition, beam-on time, and the time for couch adjustment, demonstrates the efficiency of the treatment

delivery. It was estimated that the initial setup time of 15 minutes on patient positioning for both DCAT/3D-CRT and VMAT plans. Prior to treatment delivery, the time for on-line imaging acquisition and adjustment for DCAT/3D-CRT plan was estimated to be 20 min per isocenter, including 2D planar images acquisition and following 3D cone beam computed tomography (CBCT) acquisition with OBI. For VMAT plans, the need for more accurate positioning due to the larger union of lesions is achieved by ExacTrac system, which provides six degree of freedom image guidance. It was estimated that the time for on-line imaging acquisition and adjustment with ExacTrac system and following CBCT acquisition to be 25 min for VMAT plans with single isocenter. Beam-on time could be theoretically computed by the total MU to dose rate. For DCAT/3D-CRT plans, beam-on time was computed by the total MU divided by 1000 MU/min. However, dose rate in VMAT plans changes over time based on the optimization algorithm, so that the beam-on time was estimated to be the total MU divided by the maximum dose rate, 600 MU/min. During the delivery, it takes time for therapists to go into the treatment room to adjust the couch angle between arcs in DCAT and VMAT plans, and between beams in 3D-CRT plans. It was estimated to be 1.5 min per adjustment. The total treatment time for various plans was estimated as follows:

$$\text{Treatment time}_{\text{DCAT}}\ (\text{min}) = 15 + 20 \times \text{isocenter number} + \frac{\text{MU}}{1000} + 1.5 \times \text{arc number} \tag{2.6}$$

$$\text{Treatment time}_{\text{3D-CRT}}\ (\text{min}) = 15 + 20 \times \text{isocenter number} + \frac{\text{MU}}{1000} + 1.5 \times \text{couch angle number} \tag{2.7}$$

$$\text{Treatment time}_{\text{VMAT}}\ (\text{min}) = 15 + 25 + \frac{\text{MU}}{600} + 1.5 \times \text{arc number} \tag{2.8}$$

2.5 Impact of the Distance Between Individual PTVs and VMAT Isocenter

To investigate the impact of the distance between individual PTVs and VMAT isocenter on VMAT plans, PTVs with a distance ≤ 5 cm diameter to VMAT isocenter were defined as the central group while PTVs with a distance > 5 cm to VMAT isocenter were defined as the peripheral group. Dosimetric parameters, including CI, TC, and quality of coverage for PTV were computed for plan evaluation.

3
Results

3.1 Dose Conformity, Target Coverage, and Quality of Coverage

Table 3-1 to Table 3-4 and Figure 3-1 to Figure 3-4 show the CI, TC, and quality of coverage for DCAT/3D-CRT and VMAT plans in 17 patients with different numbers of lesions. Table 3-5 summarizes these dosimetric parameters and p values.

The mean CI for DCAT/3D-CRT plans was 1.46 ± 0.21, 1.66 ± 0.44, 1.75 ± 0.28 and 1.75 ± 0.31 in patients with 5, 4, 3, and 2 lesions, respectively. The mean CI for VMAT plans was 1.38 ± 0.19, 1.43 ± 0.3, 1.49 ± 0.36, and 1.32 ± 0.2 in patients with 5, 4, 3, and 2 lesions, respectively. For patients with 5 lesions, VMAT plans have comparable conformity to DCAT/3D-CRT plans. For patients with 4, 3, and 2 lesions, VMAT were significantly more conformal than DCAT/3D-CRT plans. The improvement in CI was particularly substantial for patients with 2 lesions. CI improved from 1.75 ± 0.31 to 1.32 ± 0.2.

The mean TC for DCAT/3D-CRT plans was 99.44 ± 0.66, 99.54 ± 0.5, 99.87 ± 0.14, and 99.75 ± 0.19 in patients with 5, 4, 3, and 2 lesions, respectively. The mean TC for VMAT plans was 99.67 ± 0.29, 99.63 ± 0.47, 99.85 ± 0.2, and 99.85 ± 0.14 in patients with 5, 4, 3, and 2 lesions, respectively. There was no statistical difference in the mean TC between DCAT/3D-CRT plans and VMAT plans.

The mean quality of coverage for DCAT/3D-CRT plans was 0.96 ± 0.02, 0.93 ± 0.06, 0.97 ± 0.02, and 0.96 ± 0.01 in patients with 5, 4, 3, and 2 lesions, respectively. The mean quality of

coverage for VMAT plans was 0.97 ± 0.02, 0.97 ± 0.02, 0.99 ± 0.04, and 0.98 ± 0.02 for patients with 5, 4, 3, and 2 lesions, respectively. All VMAT plans with various lesion numbers have significantly higher quality of coverage.

Table 3-1: Comparison of dosimetric parameters for patients with 5 lesions.

	Conformity Index		Target Coverage (%)		Quality of Coverage	
	DCAT/ 3D-CRT	VMAT	DCAT/ 3D-CRT	VMAT	DCAT/ 3D-CRT	VMAT
Patient 1						
PTV 1	1.57	1.33	99.7	99.9	0.96	0.97
PTV 2	1.36	1.33	99.3	99.8	0.94	0.97
PTV 3	1.55	1.37	99.5	99.8	0.95	0.95
PTV 4	1.59	1.31	99.5	99.9	0.93	0.97
PTV 5	1.59	1.58	99.8	99.5	0.97	0.99
Patient 2						
PTV 1	1.55	1.52	99.8	99.7	0.95	0.95
PTV 2	1.68	1.15	99.9	99.2	0.95	0.96
PTV 3	1.57	1.63	99.3	99.9	0.94	0.98
PTV 4	1.37	1.65	99.8	100	0.98	1.02
Patient 3						
PTV 1	1.05	1.22	99.6	99.7	0.97	0.96
PTV 2	1.20	1.33	97.2	99.9	0.94	0.97
PTV 3	1.31	1.2	98.5	99.8	0.94	0.97
PTV 4	1.42	1.16	99.9	99.4	0.97	0.97
PTV 5	1.17	1.23	98.9	99.8	0.96	0.98
Patient 4						
PTV 1	1.47	1.18	99.7	99.7	0.96	0.97
PTV 2	1.83	1.45	99.7	99.3	0.98	0.95
PTV 3	1.22	1.8	99.9	100	0.95	1.01
PTV 4	1.48	1.3	99.4	99.4	0.98	0.96
PTV 5	1.77	1.41	100	99	0.99	0.95

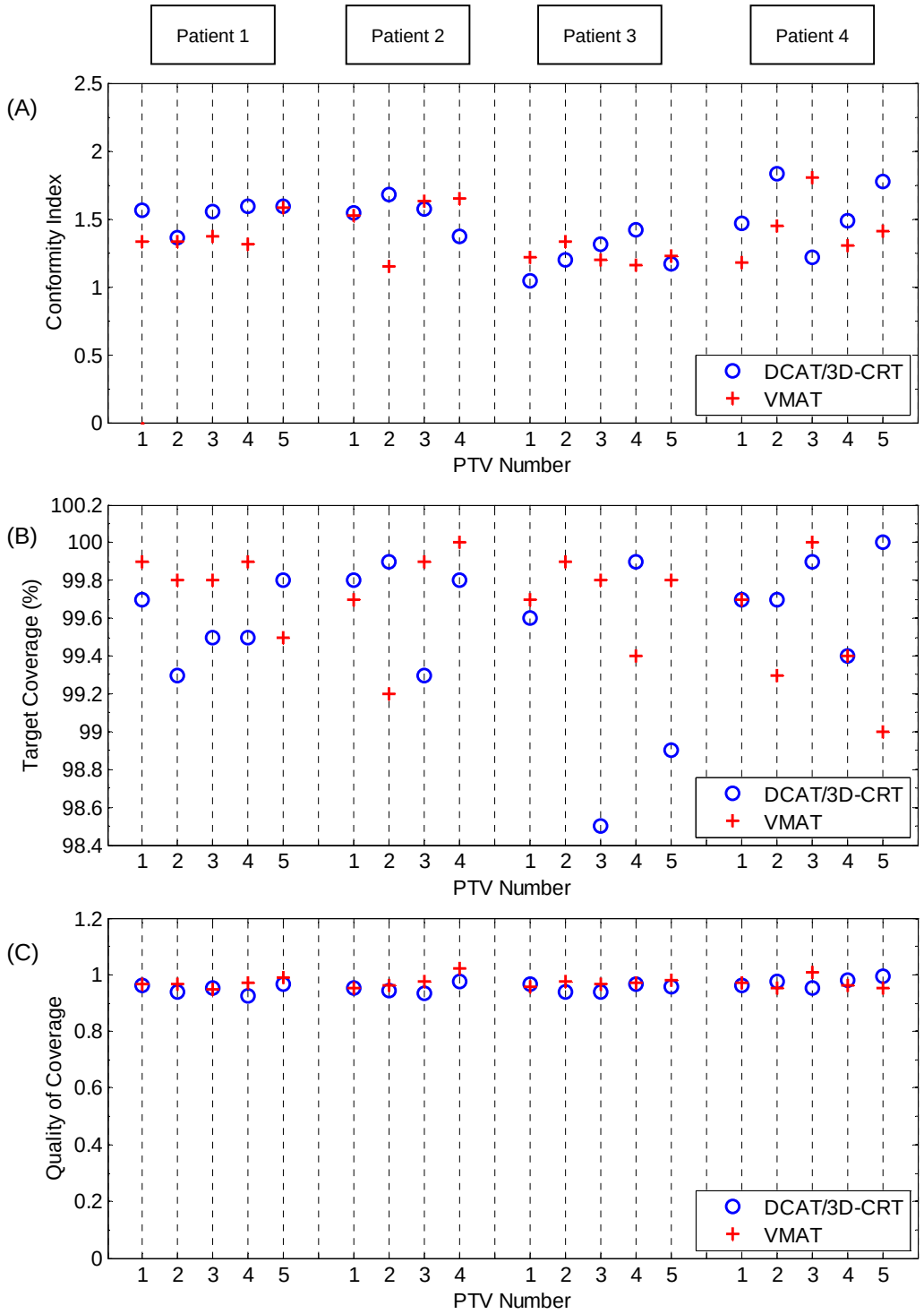

Figure 3-1: (A) Conformity index, (B) target coverage, and (C) quality of coverage for DCAT/3D-CRT and VMAT plans in patients with 5 lesions.

Table 3-2: Comparison of dosimetric parameters for patients with 4 lesions.

	Conformity Index		Target Coverage (%)		Quality of Coverage	
	DCAT/ 3D-CRT	VMAT	DCAT/ 3D-CRT	VMAT	DCAT/ 3D-CRT	VMAT
Patient 5						
PTV 1	1.41	2.06	99.4	99.5	0.92	0.91
PTV 2	2.00	1.3	99.8	100	0.95	1.01
PTV 3	2.19	1.5	99.8	100	0.97	0.98
PTV 4	1.72	1.4	99.8	100	0.96	0.99
Patient 6						
PTV 1	1.45	1.14	99.8	99.7	0.90	0.97
PTV 2	1.35	1.17	99.9	99.7	0.95	0.98
PTV 3	1.45	1.21	99.7	99.9	0.93	0.99
PTV 4	1.21	1.4	99.8	100	0.95	0.99
Patient 7						
PTV 1	1.54	1.19	99.6	99.7	0.95	0.95
PTV 2	1.53	1.24	99.6	99.8	0.95	0.94
PTV 3	1.65	1.29	99.8	99.8	0.96	0.96
PTV 4	1.52	1.44	99.8	100	0.92	0.97
Patient 8						
PTV 1	1.33	1.22	98.3	99.7	0.89	0.97
PTV 2	1.38	1.28	98.5	99.7	0.87	0.95
PTV 3	1.37	1.24	98.5	99.8	0.72	0.98
PTV 4	1.02	1.54	99.7	99.8	0.91	0.97
Patient 9						
PTV 1	2.06	1.23	99.4	98.7	0.97	0.95
PTV 2	2.08	1.55	99.7	99.7	0.96	0.98
PTV 3	1.98	1.93	99.8	98.4	0.99	0.95
PTV 4	2.95	2.19	100	98.7	1.01	0.97

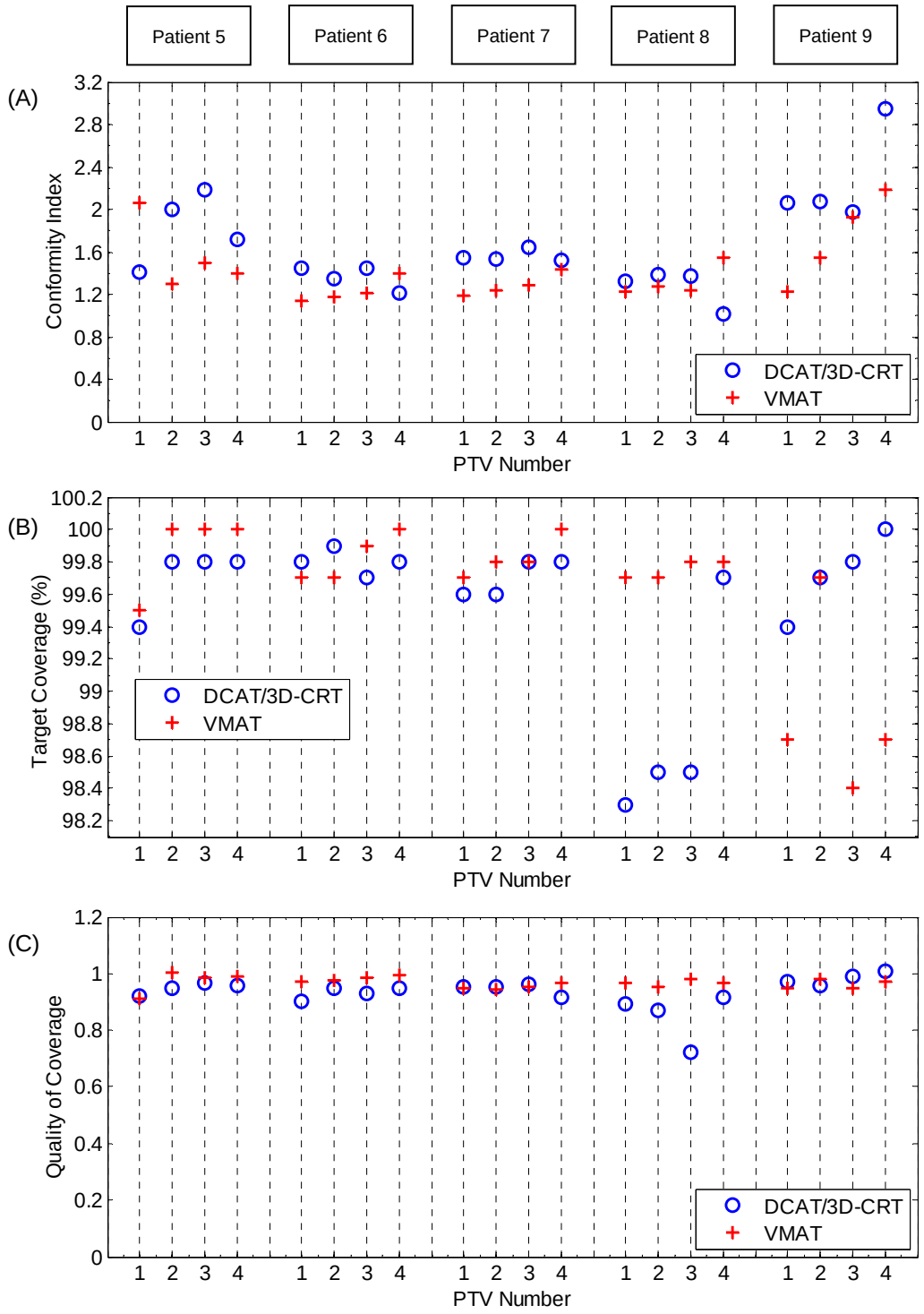

Figure 3-2: (A) Conformity index, (B) target coverage, and (C) quality of coverage for DCAT/3D-CRT and VMAT plans in patients with 4 lesions.

Table 3-3: Comparison of dosimetric parameters for patients with 3 lesions.

	Conformity Index		Target Coverage (%)		Quality of Coverage	
	DCAT/ 3D-CRT	VMAT	DCAT/ 3D-CRT	VMAT	DCAT/ 3D-CRT	VMAT
Patient 10						
PTV 1	1.43	1.67	99.7	99.7	0.96	0.97
PTV 2	1.84	1.38	99.6	99.4	0.96	0.92
PTV 3	1.37	1.29	99.8	100	0.98	1.00
Patient 11						
PTV 1	2.20	1.07	100	99.7	1.00	0.98
PTV 2	1.86	1.24	100	100	1.00	1.00
PTV 3	1.72	1.36	100	100	1.00	1.02
Patient 12						
PTV 1	1.42	1.21	99.8	99.7	0.93	0.97
PTV 2	1.60	1.35	99.8	100	0.96	1.01
PTV 3	1.68	1.89	99.8	100	0.97	1.04
Patient 13						
PTV 1	1.80	1.24	99.9	99.7	0.94	0.95
PTV 2	1.86	1.88	100	100	0.96	1.03
PTV 3	2.26	2.26	100	100	0.97	1.03

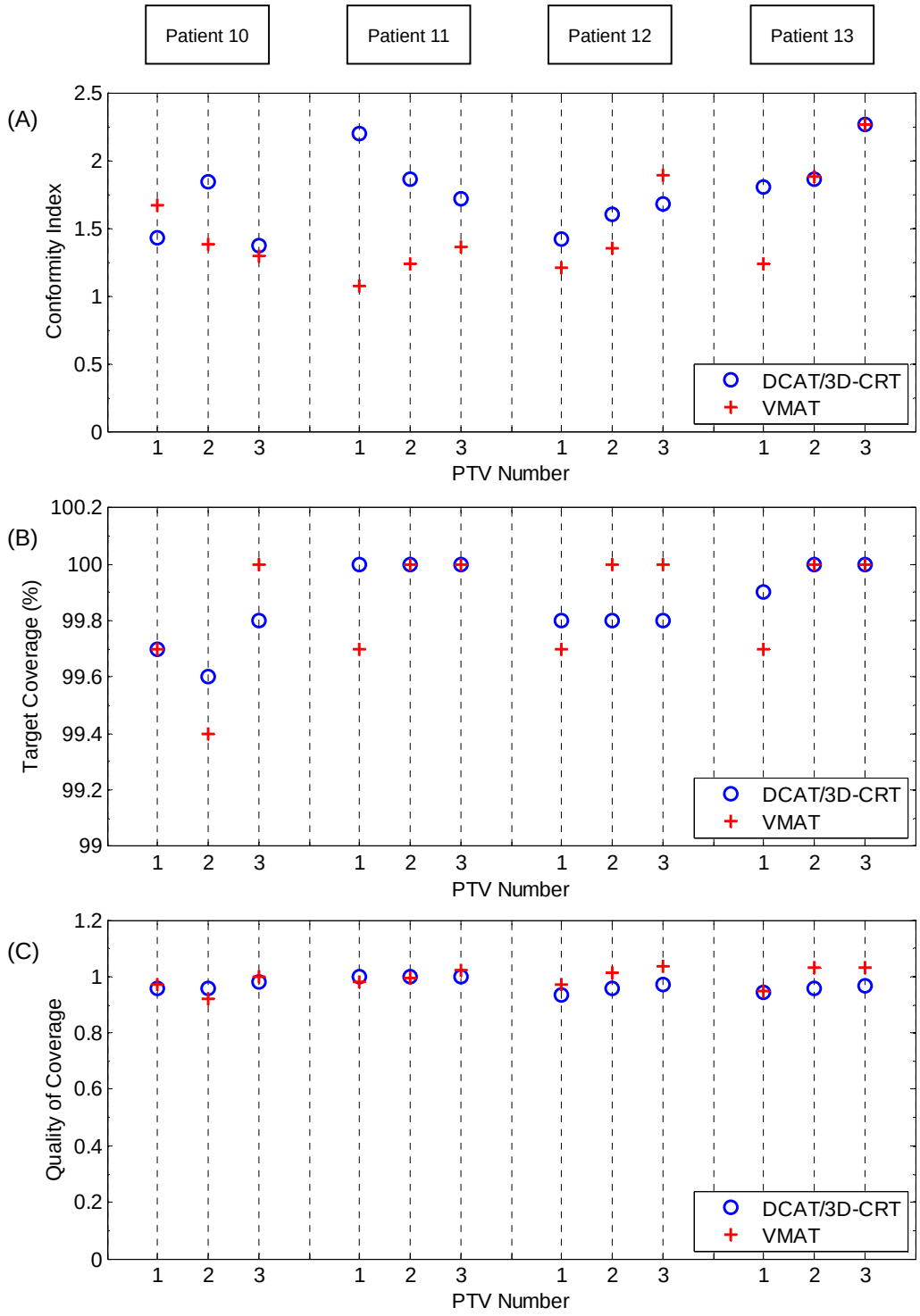

Figure 3-3: (A) Conformity index, (B) target coverage, and (C) quality of coverage for DCAT/3D-CRT and VMAT plans in patients with 3 lesions.

Table 3-4: Comparison of dosimetric parameters for patients with 2 lesions.

	Conformity Index		Target Coverage (%)		Quality of Coverage	
	DCAT/ 3D-CRT	VMAT	DCAT/ 3D-CRT	VMAT	DCAT/ 3D-CRT	VMAT
Patient 14						
PTV 1	1.68	1.12	99.7	99.7	0.94	0.96
PTV 2	1.65	1.48	99.8	100	0.97	0.99
Patient 15						
PTV 1	1.62	1.17	99.7	99.7	0.96	0.96
PTV 2	2.50	1.72	99.9	99.8	0.94	0.98
Patient 16						
PTV 1	1.52	1.28	99.4	100	0.96	1.00
PTV 2	1.57	1.36	99.6	100	0.96	1.01
Patient 17						
PTV 1	1.70	1.22	99.9	99.7	0.95	0.98
PTV 2	1.76	1.24	100	99.9	0.97	0.99

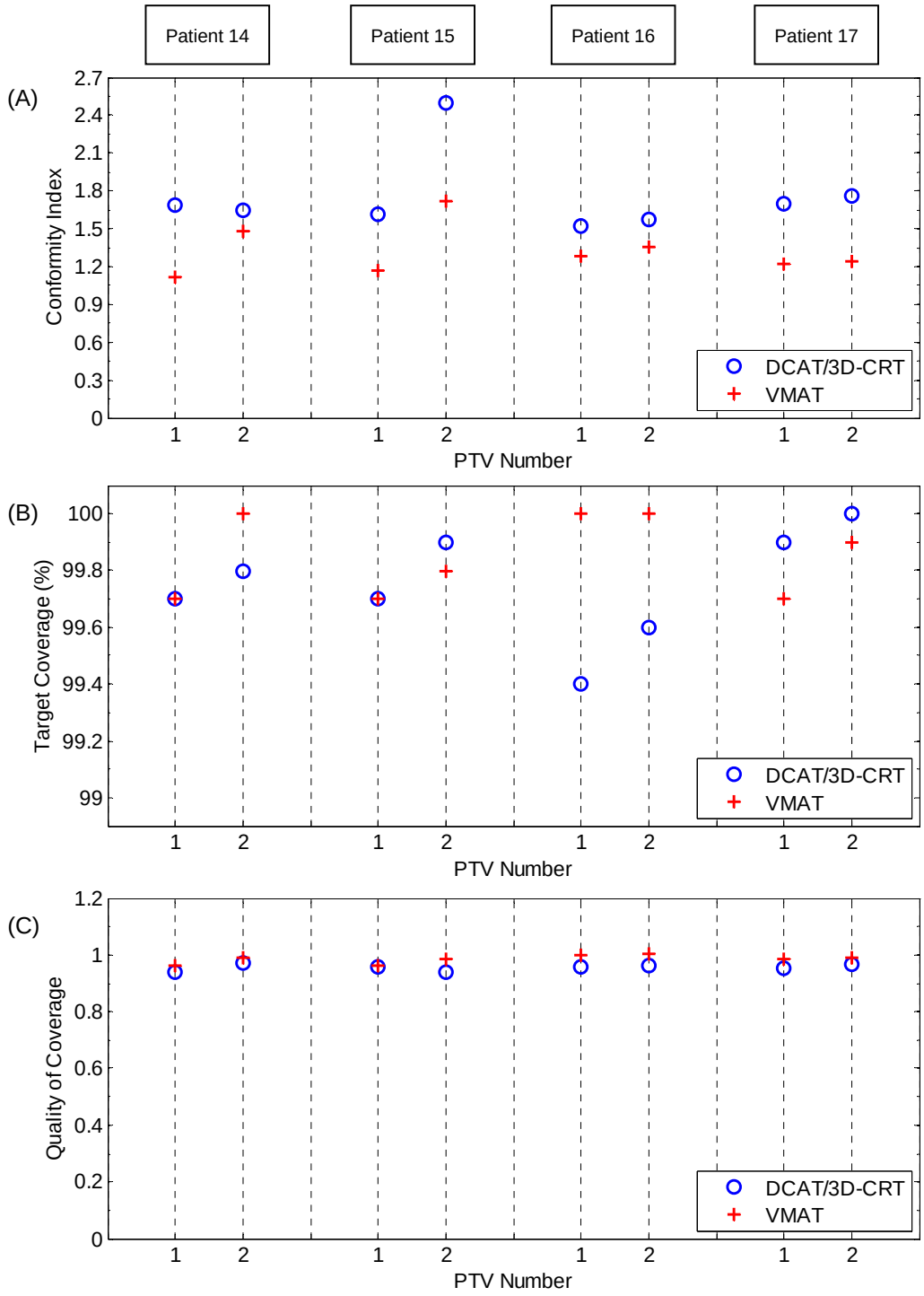

Figure 3-4: (A) Conformity index, (B) target coverage, and (C) quality of coverage for DCAT/3D-CRT and VMAT plans in patients with 2 lesions.

Table 3-5: Comparison of mean dosimetric parameters between DCAT/3D-CRT and VMAT plans in 17 patients with different numbers of lesions. The highlighted p value indicates a significant difference.

	DCAT/3D-CRT	VMAT	p value
5 lesions			
Conformity Index	1.46 ± 0.21	1.38 ± 0.19	0.19
Target Coverage (%)	99.44 ± 0.66	99.67 ± 0.29	0.24
Quality of Coverage	0.96 ± 0.02	0.97 ± 0.02	**0.04**
4 lesions			
Conformity Index	1.66 ± 0.44	1.43 ± 0.3	**0.01**
Target Coverage (%)	99.54 ± 0.5	99.63 ± 0.47	0.55
Quality of Coverage	0.93 ± 0.06	0.97 ± 0.02	**0.02**
3 lesions			
Conformity Index	1.75 ± 0.28	1.49 ± 0.36	**0.04**
Target Coverage (%)	99.87 ± 0.14	99.85 ± 0.2	0.73
Quality of Coverage	0.97 ± 0.02	0.99 ± 0.04	**0.04**
2 lesions			
Conformity Index	1.75 ± 0.31	1.32 ± 0.2	**0.0007**
Target Coverage (%)	99.75 ± 0.19	99.85 ± 0.14	0.34
Quality of Coverage	0.96 ± 0.01	0.98 ± 0.02	**0.0008**

3.2 Normal Tissue Receiving Low Dose

Table 3-6 and Figure 3-5 show the volume of the low-dose region for DCAT/3D-CRT and VMAT plans. A total of 12 out of 17 VMAT plans resulted in a larger volume of normal tissue receiving a dose of 5 Gy or greater. The mean increase of 46% in the volume of low-dose region was observed in VMAT plans. The increase in low-dose region for VMAT plans was more prominent for patients with more lesions.

Table 3-6: The volume of the low-dose region for DCAT/3D-CRT and VMAT plans. The low-dose region is defined as the volume receiving a dose of 5 Gy or greater. The values for VMAT plans were normalized to DCAT/3D-CRT plans and expressed in percentages.

	Volume of the low-dose region (cm^3)		
	DCAT/3D-CRT	VMAT	(%)
5 lesions			
Patient 1	283.89	446.83	157
Patient 2	231.88	520.58	225
Patient 3	126.31	365.35	289
Patient 4	167.83	225.55	134
4 lesions			
Patient 5	82.15	191.00	233
Patient 6	273.50	301.91	110
Patient 7	143.56	281.60	196
Patient 8	108.95	76.76	70
Patient 9	443.76	365.73	82
3 lesions			
Patient 10	112.72	156.60	139
Patient 11	64.37	61.41	95
Patient 12	119.73	188.04	157
Patient 13	120.41	111.19	92
2 lesions			
Patient 14	62.99	59.10	94
Patient 15	51.72	72.66	140
Patient 16	73.44	99.02	135
Patient 17	43.01	57.15	133
Mean ± SD			146 ± 59

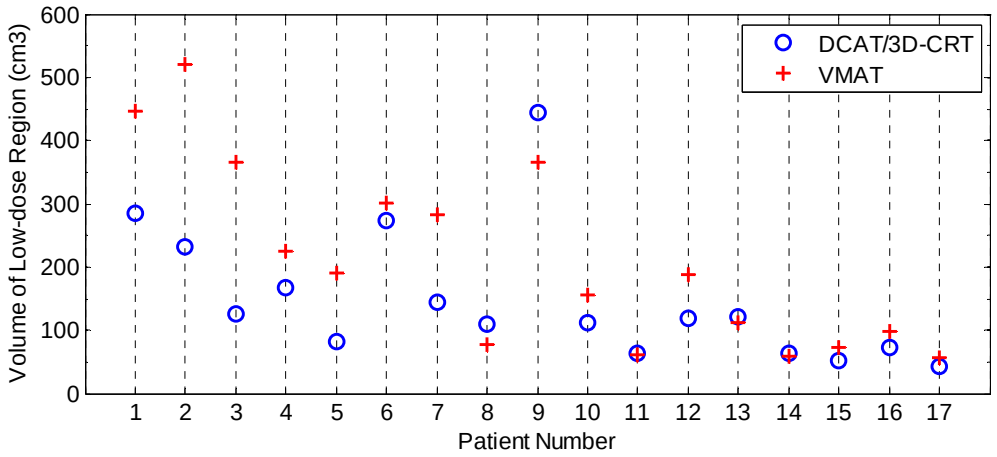

Figure 3-5: The volume of the low-dose region (volume receiving 5 Gy) for DCAT/3D-CRT and VMAT plans.

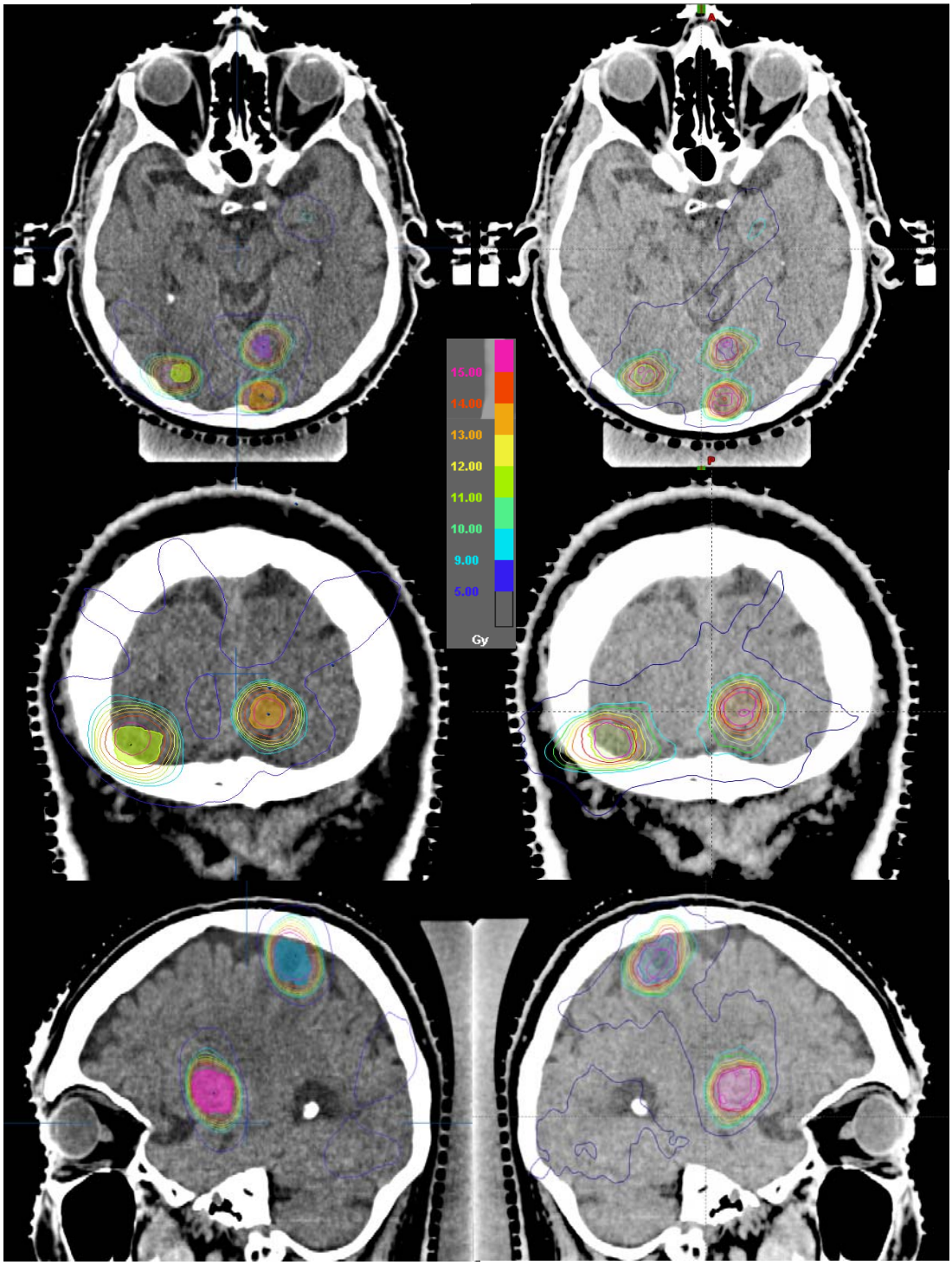

Figure 3-6: Isodose distributions for a patient with 5 lesions in DCAT/3D-CRT plans (left) and VMAT plans (right). The blue isodose lines are 5 Gy.

3.3 Treatment Delivery Efficiency

Table 3-7, Figure 3-7, and Figure 3-8 show the MU and treatment time for DCAT/3D-CRT and VMAT plans. All VMAT plans have lower MU than DCAT/3D-CRT plans except for patient 14. The mean MU decreased by 42% for VMAT plans. All VMAT plans have less treatment time than that of the DCAT/3D-CRT plans. The mean treatment time decreased by 49% for VMAT plans. Both the reduction in MU and treatment time for VMAT plans was more prominent for patients with more lesions.

Table 3-7: The monitor units and treatment time for DCAT/3D-CRT and VMAT plans. The values of monitor unit and treatment time for VMAT plans were normalized to DCAT/3D-CRT plans and expressed in percentages.

	Monitor Unit			Treatment Time (min)		
	DCAT/ 3D-CRT	VMAT	(%)	DCAT/ 3D-CRT	VMAT	(%)
5 lesions						
Patient 1	10155	4307	42.4	163	55	33.6
Patient 2	10631	6187	58.2	136	58	42.6
Patient 3	14782	5997	40.6	160	57	36.0
Patient 4	14255	4946	34.7	159	56	35.0
4 lesions						
Patient 5	10555	5015	47.5	136	56	41.2
Patient 6	11244	4579	40.7	130	55	42.3
Patient 7	12208	5090	41.7	131	56	42.7
Patient 8	7184	3481	48.5	131	53	40.8
Patient 9	8582	1166	13.6	170	46	27.3
3 lesions						
Patient 10	9242	5101	55.2	107	55	51.1
Patient 11	8383	4609	55.0	104	55	52.9
Patient 12	7955	4196	52.7	101	54	54.0
Patient 13	9159	6394	69.8	101	58	57.8
2 lesions						
Patient 14	6217	7726	124.3	73	60	82.5
Patient 15	5108	4883	95.6	75	56	74.1
Patient 16	6549	5270	80.5	74	56	76.5
Patient 17	4932	4118	83.5	72	54	75.6
Mean ± SD			58 ± 26			51 ± 17

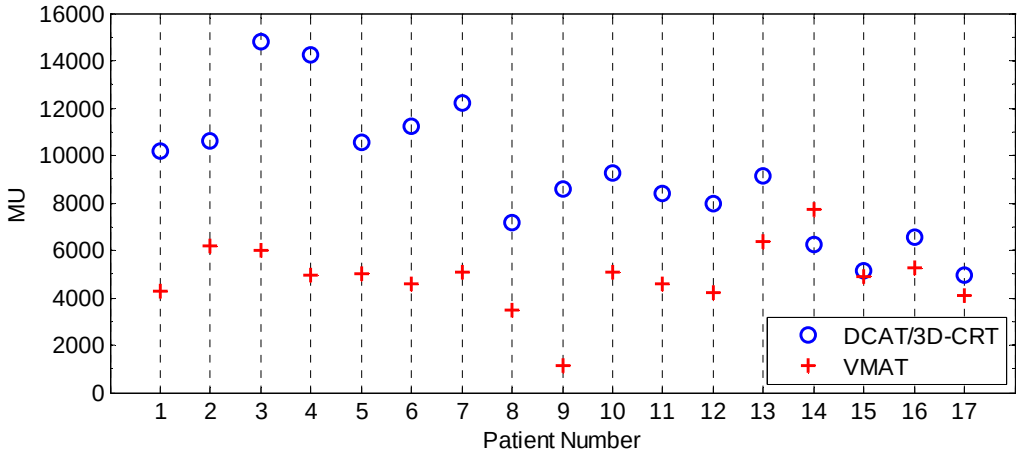

Figure 3-7: The monitor units for DCAT/3D-CRT and VMAT plans.

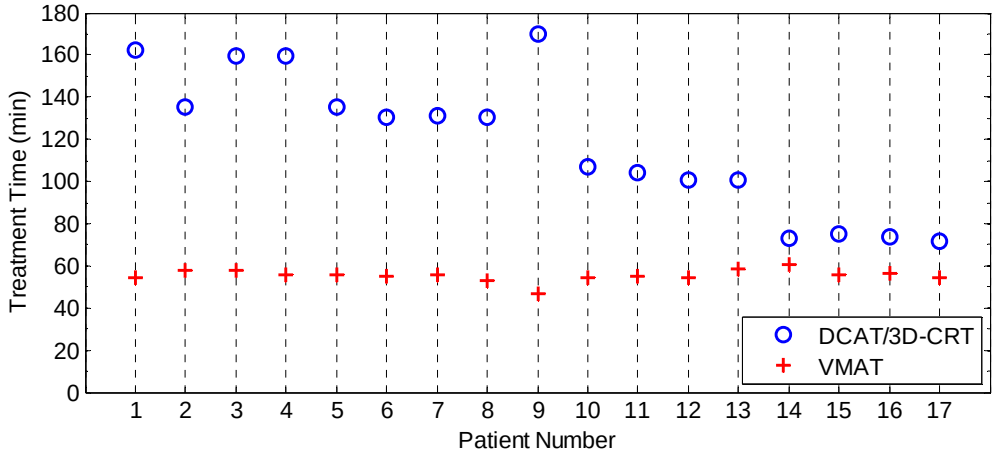

Figure 3-8: The treatment time for DCAT/3D-CRT and VMAT plans.

3.4 Impact of the Distance Between Individual PTVs and VMAT Isocenter

Among 59 PTVs, 40 PTVs were in the central group while 19 PTVs were in the peripheral group. Table 3-8 lists the mean CI, TC, quality of coverage, and p values for DCAT/3D-CRT and VMAT plans in the central and peripheral group.

In the central group, significantly higher conformity and quality of coverage were observed for VMAT plans. The mean CI was 1.64 ± 0.36 for DCAT/3D-CRT plans and 1.43 ± 0.3 for VMAT plans. The mean quality of coverage was 0.95 ± 0.05 for DCAT/3D-CRT plans and 0.98 ± 0.03 for VMAT plans. On the other hand, no significant differences were observed in the mean TC with 99.63 ± 0.4 for DCAT/3D-CRT plans and 99.72 ± 0.37 for VMAT plans.

Similar trends were shown in the peripheral group. There were significantly higher conformity and quality of coverage for VMAT plans. The mean CI was 1.59 ± 0.31 for DCAT/3D-CRT plans and 1.37 ± 0.2 for VMAT plan. The mean quality of coverage was 0.96 ± 0.02 for DCAT/3D-CRT plans and 0.97 ± 0.02 for VMAT plans. No significant differences were observed in the mean TC with 99.54 ± 0.67 for DCAT/3D-CRT plans and 99.71 ± 0.29 for VMAT plans.

Table 3-8: Comparison of dosimetric parameters for a total of 59 PTVs in the central and peripheral group between DCAT/3D-CRT and VMAT plans. The highlighted p value indicates a significant difference.

	DCAT/3D-CRT	VMAT	p value
Central (n = 40)			
Conformity Index	1.64 ± 0.36	1.43 ± 0.3	**0.0007**
Target Coverage (%)	99.63 ± 0.4	99.72 ± 0.37	0.3
Quality of Coverage	0.95 ± 0.05	0.98 ± 0.03	**0.0003**
Peripheral (n = 19)			
Conformity Index	1.59 ± 0.31	1.37 ± 0.2	**0.003**
Target Coverage (%)	99.54 ± 0.67	99.71 ± 0.29	0.36
Quality of Coverage	0.96 ± 0.02	0.97 ± 0.02	**0.03**

4
Discussion

The mean dosimetric parameters, including dose conformity, target coverage and quality of coverage for single-isocenter VMAT plans were comparable to conventional multi-isocenter DCAT/3D-CRT plans. Our results demonstrate that VMAT plans can achieve comparable conformity for patients with 5 lesions and higher conformity for patients with 2 to 4 lesions, with a substantial improvement for patients with 2 lesions. It is expected that the conformity for VMAT plans is higher than DCAT/3D-CRT plans because of beam modulation. For patients with 5 lesions, no significant difference in conformity might result from the less flexibility during the optimization. In contrast, the substantial improvement for patients with 2 lesions might result from more flexibility in optimization because of the smaller number of lesions. Similar mean target coverage, which was higher than 99% for both conventional DCAT/3D-CRT plans and VMAT plans, indicates all the plans have high target coverage. The higher mean quality of coverage observed in VMAT plans suggests that VMAT plans have higher minimum dose in the target volume compared with DCAT/3D-DRT plans.

A larger low-dose volume was observed in VMAT plans, and the increase was more prominent for patients with more lesions. This may result from less flexibility in MLC opening for VMAT plans since a fixed collimator angle was used to treat multiple lesions in this study. MLC is unable to close completely between lesions at all the different gantry angles when we try to treat multiple lesions at the same time, so the region irradiated between lesions may result in a larger low-dose volume. As the number of lesions increases, the flexibility in MLC opening is

further reduced. In addition, more MLC leakage in VMAT plans due to the wider jaw opening to cover the combined PTV may also cause this larger low-dose region. Hall et al [21] stated that a larger volume of normal tissue irradiated to low doses will increase the risk of secondary malignancy induction. The risk may be less important with respect to the palliative purpose in treatment of multiple brain metastases, but it should be considered for young patients with longer estimated lifespan [21, 25].

As expected, VMAT plans substantially reduced treatment time, and the reduction was more prominent for patients with more lesions. One of the reasons is that the number of MU for VMAT plans was greatly reduced. Since VMAT plans treated multiple lesions at each gantry angle, MU was delivered more efficiently, which resulted in a lower MU as well as the less beam-on time. In addition, single-isocenter setup requires less time for on-line imaging acquisition and couch adjustment, which also plays an important role in reducing treatment time. For patients with more lesions, the greater difference between the number of isocenters used in DACT/3D-CRT plans and VMAT plans lead to the more prominent reduction in treatment time for VMAT plans. The reduction in treatment time not only minimizes intra-fraction motion but also allows more time for on-line imaging acquisition. However, it should be noted that the treatment time for VMAT plans was estimated with maximum constant dose rate of 600 MU/min. Therefore, the actual treatment time was somehow underestimated.

The distance between individual PTVs and VMAT isocenter has no impact on VMAT plans. The higher conformity and quality of coverage for VMAT plans compared with DCAT/3D-CRT plans were consistent with the results from the evaluation in which the patients were grouped according to the number of lesions. This suggests that the dosimetric performance of single-isocenter VMAT plans is comparable to DCAT/3D-CRT without compromising individual PTVs with different distances to VMAT isocenter.

The employment of the union of PTVs also makes localization much more important in this

SRS treatment with single-isocenter VMAT. For conventional DCAT/3D-CRT plans with multiple isocenters, beams are focused to a small region. On the other hand, the union of PTVs is relatively large, and most of the PTVs are in different planes in single-isocenter VMAT plans, so the positioning error may cause a great discrepancy between the planned dose and delivered dose. Imaging guidance systems can provide further verification of positioning before treatment delivery. For example, ExacTrac system is employed at Duke University Medical Center to provide six degrees of freedom image guidance, correcting patient rotations in pitch, roll, and yaw as shown in Figure 4-1.

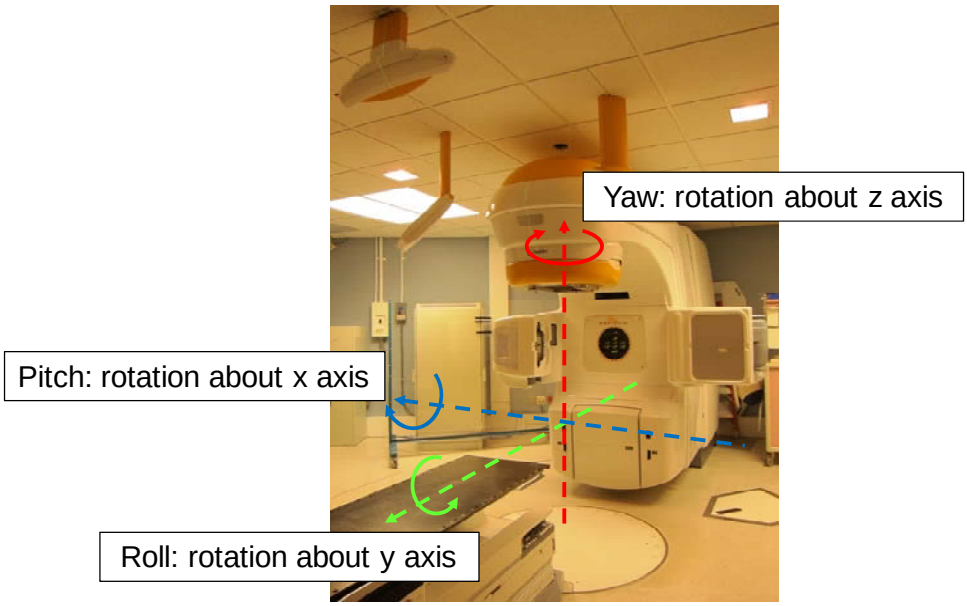

Figure 4-1: Illustration of pitch, roll, and yaw rotations. Rotation about x axis is pitch; rotation about y axis is roll; rotation about z axis is yaw.

5
Conclusion

Our investigation of dosimetric performance and treatment delivery efficiency suggests that single-isocenter VMAT is promising for SRS in the treatment of multiple brain metastases. Single-isocenter VMAT is able to achieve comparable dose conformity, target coverage, and quality of coverage to conventional DCAT and 3D-CRT plans. However, single-isocenter VMAT might result in a larger low-dose region. With single-isocenter VMAT, treatment delivery efficiency can be substantially improved. Total treatment time is substantially reduced because of the lower MU and the employment of single isocenter. In addition, the distance between individual PTVs and VMAT isocenter has no impact on VMAT plans.

Bibliography

1. I. T. Gavrilovic and J. B. Posner, Brain metastases: epidemiology and pathophysiology. *J Neurooncol* 2005, 75(1):5-14.

2. M. E. Linskey, et al., The role of stereotactic radiosurgery in the management of patients with newly diagnosed brain metastases: a systematic review and evidence-based clinical practice guideline. *J Neurooncol* 2010, 96(1):45-68.

3. L. S. Chin and W. F. Regine, *Principles and Practice of Stereotactic Radiosurgery.* 1st edition, 2008. Springer.

4. A. F. Eichler, et al., The biology of brain metastases-translation to new therapies. *Nat Rev Clin Oncol* 2011, 8(6):344-356.

5. R. Kamath, et al., Initial clinical experience with frameless radiosurgery for patients with intracranial metastases. *Int J Radiat Oncol Biol Phys* 2005, 61(5):1467-72.

6. A. F. Eichler and J. S. Loeffler, Multidisciplinary management of brain metastases. *The Oncologist* 2007, 12(7):884-98.

7. D. Rades, et al., Whole brain radiotherapy plus stereotactic radiosurgery (WBRT+SRS) versus surgery plus whole brain radiotherapy (OP+WBRT) for 1-3 brain metastases: results of a matched pair analysis. *Eur J Cancer* 2009, 45(3):400-4.

8. G. M. Clark, et al., Feasibility of Single-Isocenter Volumetric Modulated Arc Radiosurgery for Treatment of Multiple Brain Metastases. *Int J Radiat Oncol Biol Phys* 2010, 76(1):296-302.

9. E. Shaw, et al., Single dose radiosurgical treatment of recurrent previously irradiated primary brain tumors and brain metastases: final report of RTOG protocol 90-05. *Int J Radiat Oncol Biol Phys* 2000, 47(2):291-8.

10. K. Chan, Stereotactic radiosurgery for intracranial pathology: A review of treatment techniques and results. *Hong Kong Med J* 1996, 2:297-303.

11. F. M. Khan, *The Physics of Radiation Therapy*, 2010. Lippincott Williams & Wilkins, a Wolters Kluwer business.

12. Z. Chang, et al., Six degree-of-freedom image guidance for frameless intra-cranial stereotactic radiosurgery with kilo-voltage cone-beam CT. *J Nucl Med Radiat Ther* 2010, 1:101.

13. S. H. Benedict, et al., Anniversary Paper: The role of medical physicists in developing stereotactic radiosurgery. *Med Phys* 2008, 35(9):4262-77.

14. S. P. Collins, et al., CyberKnife® radiosurgery in the treatment of complex skull base tumors: analysis of treatment planning parameters. *Radiat Oncol* 2006, 1:46.

15. R. Jeraj, et al., Radiation characteristics of helical tomotherapy. *Med Phys* 2004, 31(2):396-404.

16. B. J. Gerbi, et al., Linac-based stereotactic radiosurgery for treatment of trigeminal neuralgia. *J Appl Clin Med Phys* 2004, 5(3):80-92.

17. T. D. Solberg, et al., Dynamic arc radiosurgery field shaping: a comparison with static field conformal and noncoplanar circular arcs. *Int J Radiat Oncol Biol Phys* 2001, 49(5):1481-91.

18. M. Ding, et al., Comparative dosimetric study of three-dimensional conformal, dynamic conformal arc, and intensity-modulated radiotherapy for brain tumor treatment using Novalis system. *Int J Radiat Oncol Biol Phys* 2006, 66(4, Supplement):S82-S86.

19. G. Grebe, et al., Dynamic arc radiosurgery and radiotherapy: Commissioning and verification of dose distributions. *Int J Radiat Oncol Biol Phys* 2001, 49(5):1451-60.

20. D. Verellen, et al., Considerations on treatment efficiency of different conformal radiation therapy techniques for prostate cancer. *Radiother Oncol* 2002, 63(1):27-36.

21. E. J. Hall and C. S. Wuu, Radiation-induced second cancers: the impact of 3D-CRT and IMRT. *Int J Radiat Oncol Biol Phys* 2003, 56(1):83-8.

22. K. Otto, Volumetric modulated arc therapy: IMRT in a single gantry arc. *Med Phys* 2008, 35(1):310-7.

23. D. M. Shepard, et al., Direct aperture optimization: A turnkey solution for step-and-shoot IMRT. *Med Phys* 2002, 29(6):1007-18.

24. C. Audet, et al., Evaluation of volumetric modulated arc therapy for cranial radiosurgery using multiple noncoplanar arcs. *Med Phys* 2011, 38(11):5863-72.

25. H. A. Wolff, et al., Single fraction radiosurgery using Rapid Arc for treatment of intracranial targets. *Radiat Oncol* 2010, 5:77.

26. M. Schulder, *Handbook of Stereotactic and Functional Neurosurgery*, 2003. Informa Healthcare.

27. L. Feuvret, et al., Conformity index: a review. *Int J Radiat Oncol Biol Phys* 2006, 64(2):333-42.

28. N. J. Lomax and S. G. Scheib, Quantifying the degree of conformity in radiosurgery treatment planning. *Int J Radiat Oncol Biol Phys* 2003, 55(5):1409-19.